Inorganic Chemistry

Article

pubs.acs.org/IC

Family of Defect-Dicubane Ni_4Ln_2 (Ln = Gd, Tb, Dy, Ho) and Ni_4Y_2 Complexes: Rare Tb(III) and Ho(III) Examples Showing SMM Behavior

Lang Zhao,[†,‡] Jianfeng Wu,[†] Hongshan Ke,[†] and Jinkui Tang*[,†]

[†]State Key Laboratory of Rare Earth Resource Utilization, Changchun Institute of Applied Chemistry, Chinese Academy of Sciences, Changchun, 130022, China

[‡]State Key Laboratory of Inorganic Synthesis and Preparative Chemistry, College of Chemistry, Jilin University, Changchun 130012, China

Supporting Information

ABSTRACT: Reactions of Ln^{III} perchlorate (Ln = Gd, Tb, Dy, and Ho), $NiCl_2·6H_2O$, and a polydentate Schiff base resulted in the assembly of novel isostructural hexanuclear Ni_4Ln_2 complexes [Ln = Gd (**1**), Tb (**2**), Dy (**3**), Ho (**4**)] with an unprecedented 3d−4f metal topology consisting of two defect-dicubane units. The corresponding Ni_4Y_2 (**5**) complex containing diamagnetic Y^{III} atoms was also isolated to assist the magnetic studies. Interestingly, complexes **2** and **3** exhibit SMM characteristics and **4** shows slow relaxation of the magnetization. The absence of frequency-dependent in-phase and out-of-phase signals for the Ni−Y species suggests that the Ln ions' contribution to the slow relaxation must be effectual as previously observed in other Ni−Dy samples. However, the observation of χ'' signals with zero dc field for the Ni−Tb and Ni−Ho derivatives is notable. Indeed, this is the first time that such a behavior is observed in the Ni−Tb and Ni−Ho complexes.

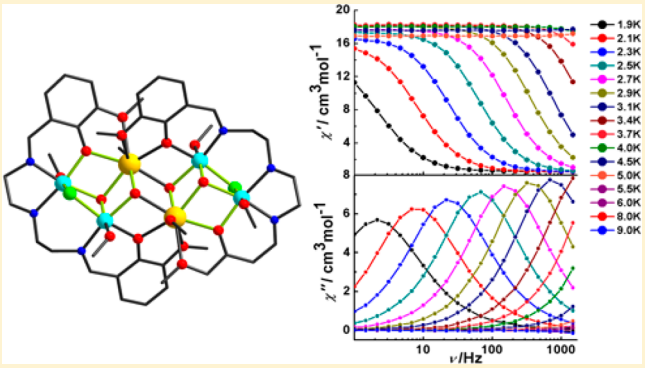

INTRODUCTION

Polymetallic complexes have attracted great attention because of their wide promising applications in many significant areas such as physics, chemistry, and materials science.[1−3] For instance, homo- and heteropolynuclear complexes are of high interest by virtue of their importance as magnetic materials, such as molecular nanomagnets,[4] offering the possibility to test the fundamental questions in physics, such as quantum tunneling and quantum phase interference, as well as their applications ranging from quantum computing[5] and high-density memory storage devices[6] to magnetic refrigeration.[7] 3d−4f complexes are of interest because, in most cases, single ion anisotropy can often be ensured. However, the zero-field splitting of the M_J states in 4f SMMs usually results in complex patterns with multiple maxima and minima instead of a simple parabola, as seen for 3d-based SMMs, between the energetically lowest M_J states. In this context, many 3d/4f systems, particularly those containing Cu−Ln,[8] Mn−Ln,[9] Fe−Ln,[10] and Co−Ln[11] systems, are widely investigated. However, in contrast, there are few examples known for Ni−Ln[12−14] based clusters exhibiting SMM behavior.[15] The isolation of new Ni−Ln complexes will help our understanding of these types of complexes, in regard to their synthesis and magnetic analysis.

The construction of 3d−4f systems is usually facilitated by the use of suitable compartmental ligands containing appropriate pockets that can bind different metal ions.[16] Recently, we have employed (*E*)-2-(2-hydroxy-3-methoxybenzylideneamino)phenol in Ni−Ln cluster chemistry, and a family of Ni_4Ln_2 clusters consisting of two Ni_2LnO_4 defective cubanes with unusual structural features and magnetic properties were synthesized, where slow magnetic relaxation was observed for the Ni_4Dy_2 species.[13] To assemble novel heterometallic polynuclear complexes, we focused our research efforts on a Schiff base ligand, N_1,N_3-bis(3-methoxysalicylidene) diethylenetriamine (H_2L, Scheme S1, Supporting Information). This ligand is a compartmental type ligand and has two different coordination sites; the inner site (N_3O_2, two amide, one imine, and two phenol functions) showing preference for 3d metal ions and the outer site (O_2O_2, two phenol groups and two oxygen atoms of the methoxy groups) having preference for hard, oxophilic 4f metal ions. It is noteworthy that Long and co-workers synthesized an exchange-coupled Dy_2 complex that behaves as an SMM with a very high anisotropy barrier value of 76 K using this kind of Schiff base ligand.[17] Although some homometallic complexes and a Co_2Dy_2 complex based on H_2L have been previously reported in the literature by our group[18] and others,[19] we recently employ it in mixed Ni−Ln cluster chemistry, and a series of Ni_4Ln_2 hexanuclear complexes were synthesized for the first time by using this ligand. We herein report the synthesis, characterization, and detailed magnetic properties of a series of

Received: December 3, 2013
Published: March 24, 2014

   dx.doi.org/10.1021/ic402973g | *Inorg. Chem.* 2014, 53, 3519−3525

isostructural hexanuclear Ni_4Ln_2 complexes [Ln = Gd (**1**), Tb (**2**), Dy (**3**), Ho (**4**)] with an unprecedented 3d−4f metal topology comprising two defect-dicubane units. The corresponding Ni_4Y_2 (**5**) complex containing diamagnetic Y^{III} atoms was also isolated to assist the magnetic studies. Interestingly, complexes **2** and **3** exhibit SMM characteristics and **4** shows slow relaxation of the magnetization. The observation of χ''_M signals with zero dc field for the Ni−Tb and Ni−Ho derivatives is notable while the absence of frequency-dependent signals for the Ni−Y complex indicates that the contribution of 4f ions to the anisotropy must be effectual. If such a behavior was reported previously for other Ni−Dy samples,[15] it is indeed observed for the first time in the Ni−Tb and Ni−Ho complexes.

EXPERIMENTAL SECTION

Physical Measurements. All chemicals purchased were analytical reagent grade and used as received. Elemental analysis (C, H, and N) were performed on a PerkinElmer 2400 analyzer. IR spectra were recorded with samples prepared as KBr disks in the 4000−300 cm^{-1} range on a PerkinElmer Fourier transform infrared spectrophotometer.

X-ray Crystal Structure Determinations. Single-crystal X-ray data for complexes **1**−**5** were collected at 185(2) K on a Bruker Apex II CCD diffractometer equipped with graphite-monochromatized Mo−Kα radiation (λ = 0.71073 Å). The structures were solved by direct methods and refined by full-matrix least-squares methods on F^2 using SHELXTL-97. All non-hydrogen atoms determined from the difference Fourier maps were refined anisotropically. Hydrogen atoms were placed geometrically and refined using a riding model. Crystallographic data are listed in Table S1 (Supporting Information). CCDC 972379−972383 contain the supplementary crystallographic data for this paper. These data can be obtained free of charge from The Cambridge Crystallographic Data Centre via www.ccdc.cam.ac.uk/data_request/cif.

Magnetic Measurements. Variable-temperature magnetic susceptibility measurements were carried out using a Quantum Design MPMS-XL7 SQUID magnetometer equipped with a 7 T magnet in the temperature range of 1.9−300 K with an external magnetic field of 1000 Oe. Diamagnetic corrections were made with the Pascal's constants for all the constituent atoms as well as the contributions of the sample holder.

Preparation of Ligand H_2L. The Schiff base ligand H_2L was prepared according to the reported procedure.[19a] Diethylenetriamine (2.575 g, 25 mmol) and *o*-vanillin (7.6 g, 50 mmol) were mixed in ethanol (100 mL) and then heated at reflux for 5 h. The solvent was evaporated under reduced pressure to give H_2L as an orange oil. IR (KBr, cm^{-1}): 3438 (br), 1629 (S), 1469 (S), 1255 (m), 1080 (w), 964 (w), 734 (S). Elemental analysis (%) calcd: C, 64.85; H, 6.53; N, 11.34; found: C, 64.74; H, 6.87; N, 11.37.

Synthesis of Complexes 1−5. $Ln(ClO_4)_3{\cdot}6H_2O$ (Ln = Gd, Tb, Dy, Ho, Y) (0.15 mmol) was dissolved in CH_3OH/CH_2Cl_2 (5 mL/10 mL), followed by the addition of H_2L (0.2 mmol) and $NiCl_2{\cdot}6H_2O$ (0.3 mmol). Then triethylamine (0.57 mmol, 0.08 mL) was added after 0.5 h, and the resulting mixture was stirred for 3 h. Pale green block-shaped single crystals, suitable for X-ray diffraction analysis, were isolated after 6 days.

RESULTS AND DISCUSSION

Synthetic Aspects. N_1,N_3-bis(3-methoxysalicylidene) diethylenetriamine ligand (H_2L) was prepared by the Schiff base condensation of *o*-vanilin and diethylenetriamine. $Ln(ClO_4)_3{\cdot}6H_2O$ (Ln = Gd, Tb, Dy, Ho) was reacted with H_2L in a 3:4 ratio in the presence of $NiCl_2{\cdot}6H_2O$. By using triethylamine as the base in a $MeOH/CH_2Cl_2$ 1:2 ratio mixture, the hexanuclear 3d−4f complexes $\{[Ln_2Ni_4L_2Cl_2(OH)_2(CH_3O)_2(CH_3OH)_6]Cl_2(ClO_4)_2(CH_3OH)_2{\cdot}(H_2O)_2\}$ (Ln = Gd (**1**), Tb (**2**), Dy (**3**)) and $\{[Ho_2Ni_4L_2Cl_2(OH)_4(CH_3OH)_6]Cl_2(ClO_4)_2(CH_3OH)_2{\cdot}(H_2O)_2\}$ (**4**) could be isolated as single crystalline material. To probe the magnetic behavior of 3d−4f systems, $\{[Y_2Ni_4L_2Cl_2(OH)_4(CH_3OH)_6]Cl_2(ClO_4)_2(CH_3OH)_2{\cdot}(H_2O)_2\}$ (**5**) was synthesized to exclude the lanthanide anisotropy and the 4f contribution, but all attempts to substitute Ni with Zn were unsuccessful. Those reactions all gave noncrystalline materials that could not be further characterized. Complexes **1**−**3** crystallize in the triclinic space group $P\bar{1}$, whereas complexes **4**−**5** crystallize in the monoclinic space group $P2_1/c$. The complexes are similar to each other, but having two bridging methanol molecules connecting the Ln^{III} and Ni^{II} metal ions for complexes **1**−**3** instead of two hydroxyl groups for complexes **4**−**5**. The structure of **3** will be described as representative of the whole series.

Crystal Structures. The crystal structure consists of the entities $[Dy_2Ni_4L_2Cl_2(OH)_2(CH_3O)_2(CH_3OH)_6]^{4+}$, Cl^-, and ClO_4^- as counteranions, CH_3OH, and H_2O as the solvent molecule. A perspective view of the hexanuclear portion is depicted in Figure 1. The core of the structure can be described

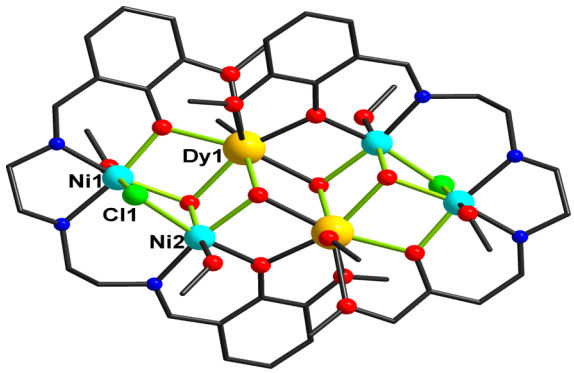

Figure 1. Molecular structure of **3** highlighting the $[Ni_2DyO_3Cl]$ heterometallic defective cubane subunits in bright green lines. The noncoordinated solvent molecules and H atoms are omitted for clarity.

as two Ni_2DyO_3Cl defective cubane subunits held together by two hydroxyl groups and two phenoxo bridging oxygen atoms (Figure 2a). Each Ni_2DyO_3Cl subunit is made of two nickel ions and one dysprosium ion arranged as a defective cubane with one missing vertex where the three metal ions are linked to each other by means of one phenoxo group, one hydroxyl group, one methanol molecule, and one chloride anion. The eight-coordinated environment of Dy1 is completed by two phenolic bridging oxygen atoms and two methoxy oxygen atoms from the ligand L, two μ_3-OH and two alcoholic oxygen atoms of the methanol molecules, close to a distorted square-antiprismatic geometry with O_8 coordination sites (Figure 2b). Dy1 and Dy1a are double-bridged by two μ_3-O atoms from two μ_3-OH to form a Dy_2O_2 rhombus with angles of 110.54(33)° and 69.46(29)° for Dy−O−Dy and O−Dy−O, respectively. The nickel ions in the N_2O_3Cl/NO_4Cl surrounding are six coordinated with the coordination polyhedron of distorted octahedral geometry. The N_2O_2 donor atoms derived from two imines, and one phenoxo group from one L ligand and one μ_3-OCH_3 ligand reside in the equatorial positions of Ni1, while one alcoholic oxygen atom of the methanol molecule and one chloride are placed in the axial positions (Figure 2c). The equatorial plane of Ni2 is composed of NO_3 atoms derived from one imine, one μ_3-hydroxyl group, one μ_3-OCH_3 ligand, and one alcoholic oxygen of the methanol as well as the axial

dx.doi.org/10.1021/ic402973g | Inorg. Chem. 2014, 53, 3519−3525

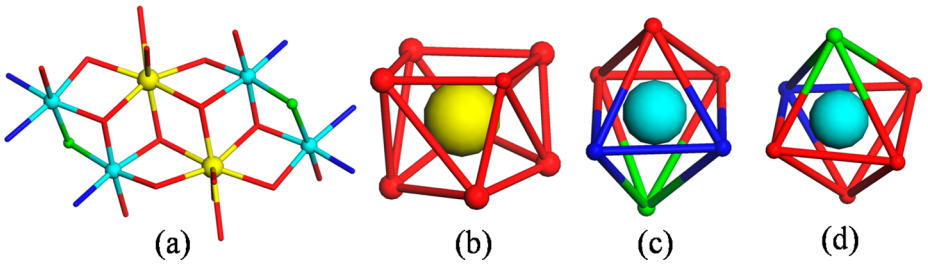

Figure 2. (a) Coordination environment of nickel and dysprosium in $[Dy_2Ni_4L_2Cl_2(OH)_2(CH_3O)_2(CH_3OH)_6]^{4+}$ (**3**). (b) Distorted square antiprismatic environment around the Dy^{III} metal ion in **3**. (c) Distorted octahedral environment around the Ni1 atom in **3**. (d) Distorted octahedral environment around the Ni2 atom in **3**: Dy (yellow), Ni (light blue), Cl (green), N (blue), O (red).

positions are occupied by one phenoxo group from one L ligand and one chloride anion (Figure 2d). The Ni−O and Ni−N bond lengths cover ranges of 1.979(2)−2.036(2) and 1.960(3)−2.166(3) Å, which are similar to the values reported in the literature. The Ni−Cl bond length is 2.465(2) Å, significantly longer than the distances of Ni−O and Ni−N. The value of the Ni1···Ni2 separation is 3.4221(16) Å. The Ni1−O5−Ni2 angle is 103.33(5)°, which is larger than the Ni1−Cl2−Ni2 angle (84.59(5)°). Ni−N, Ni−O, and Ni−Cl bond distances and the coordination environment are in line with a high-spin state of the Ni^{II} ion ($S = 1$). Two Ni ions are linked through one μ_3-OCH_3 ligand and one chloride anion toward the central Dy ion, resulting in a Ni_2DyO_3Cl defective cubane, which are further connected by two hydroxyl groups and two phenolic bridging oxygen atoms to adjacent cubane, resulting in a $Ni_4Dy_2O_8Cl_2$ core with two edge-to-edge Ni_2DyO_3Cl defective cubanes. Ni−O(i)−Dy angles are 106.2(1)° and 107.3(1)°, and the Ni−Dy distance is 3.4410(6) Å. The H_2L ligand wrapped around two Dy ions and two Ni ions with the inner N_3O_2 donors coordinating two Ni ions, while the outer O_4 donors coordinate with two Dy ions, which consolidates this Ni_4Dy_2 cluster.

It is also interesting to compare the series of Ni_4Ln_2 complexes previously reported by our group[13] with the one described herein. The reported complex[13] contains four Ni ions linked by two μ_3-OH and two phenoxo groups that lie in the central of the metal core, and the two Ln ions lie in the two edges of the metal core. While all the Ni_4Ln_2 species described in this work can be viewed that two Dy ions linked by two μ_3-OH are in the central of the metal core, and the two pairs of Ni ions lie in the two edges of the metal core. Our Ni_4Ln_2 shows a similar arrangement of metal cores as those reported in the literature,[12] but the two Ln ions are held together by two bridged μ_3-OH in our complexes instead of two bridged carboxyl groups as observed elsewhere. Such differences will affect the magnetic behavior of these complexes.

Magnetic Properties. The static magnetic susceptibilities of the four Ni−Ln complexes **1**−**4** (Ln = Gd, Tb, Dy, Ho, Figure 3) and **5** (Y_2Ni_4, Figure 4) were collected in the temperature range of 2−300 K in an applied magnetic field of 1000 Oe. It is generally known that the lanthanide anisotropy can be excluded by using isotropic Gd ions, and the 4f contribution can be removed by using diamagnetic Y ions. Hence, complexes **1** and **5**, which contain Gd ions and Y ions, respectively, have been prepared. In complex **5**, the four Ni(II) ions are linked by the diamagnetic Y(III) ion, resulting in a pair of magnetically isolated dinuclear Ni_2 units. The molar magnetic susceptibility product ($\chi_M T$) of **5** at room temperature is 5.61 $cm^3\ mol^{-1}$ K, which is slightly higher than the

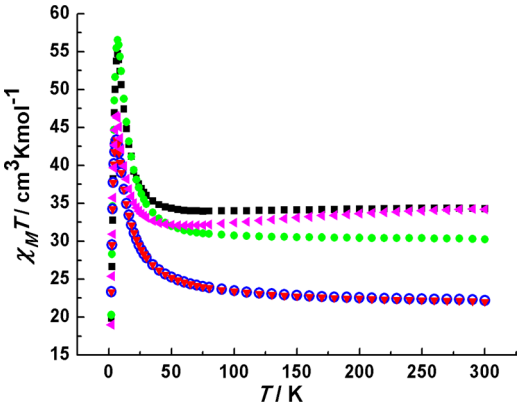

Figure 3. Temperature dependence of the $\chi_M T$ products at 1000 Oe for complexes **1** (red), **2** (green), **3** (black), and **4** (purple). The blue circles correspond to the calculated behavior of complex **1** (see the text for details).

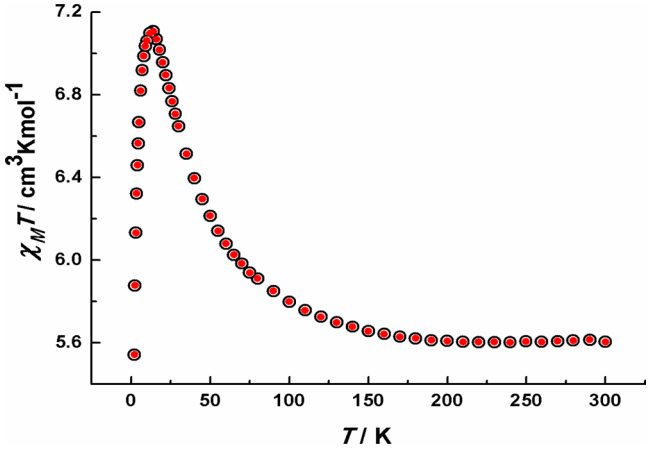

Figure 4. Temperature dependence of the $\chi_M T$ product at 1000 Oe for complex **5** (red). The black circles correspond to the calculated behavior (see the text for details).

expected value for the presence of four noninteracting Ni(II) ions ($S = 1$, if $g = 2$). On cooling, a gradual $\chi_M T$ increase to 5.65 $cm^3\ mol^{-1}$ K (150 K), followed by an abrupt increase, up to 7.10 $cm^3\ mol^{-1}$ K at 15 K, and then an abrupt decrease to 5.54 $cm^3\ mol^{-1}$ K at 2 K were observed. The curve indicates that the exchanges within complex **5** are dominated by ferromagnetic interactions between the Ni(II) ions. The decrease at low temperature is probably due to intermolecular antiferromagnetic interaction, to the presence of zero-field splitting (ZFS), or to a combined effect of the above two factors. Thus, to simulate the magnetic data, we can treat the model as two

dx.doi.org/10.1021/ic402973g | Inorg. Chem. 2014, 53, 3519−3525

isolated dimers of Ni(II) ions with the Hamiltonian of $H = -2J_1(S_{Ni1}\cdot S_{Ni2}) - 2[D(Sz^2 - 1/3S(S+1)) + g\mu_B HS_z]$ using the MAGPACK[20] program, where J_1 represents the exchange parameter between the Ni(1)···Ni(2) and Ni(1)#1···Ni(2)#1 ions and D accounts for axial single-ion zero-field splitting (ZFS) of the Ni(II) ions. A fit to the experimental data gives $J_1 = 2.78$ cm^{-1}, $D = 5.16$ cm^{-1}, and $g = 2.28$ with $R = 3.79 \times 10^{-3}$ that further indicated ferromagnetic coupling between nickel(II) ions. The magnetization measurement for complex **5** at 1.9 K (Figure S1, Supporting Information) shows a rapid increase of the magnetization and eventually reaches 8.4 μ_B at 1.9 K and 7 T, in line with the presence of ferromagnetic interactions in this system.

For the analogous gadolinium complex **1**, the two Ni^{II} ions are linked through the paramagnetic Gd^{III} ion that can mediate the magnetic interactions between the two types of metal ions. The $\chi_M T$ vs T plot shows similar thermal behavior to that of **5**. The observed $\chi_M T$ value at 300 K of 22.20 cm^3 mol^{-1} K for **1** is slightly higher than the calculated value of 19.75 cm^3 mol^{-1} K for two noninteracting Gd^{III} ($S = 7/2$, $C = 7.875$ cm^3 mol^{-1} K) and four high-spin Ni^{II} ($S = 1$, if $g = 2$) ions. On cooling, the $\chi_M T$ value increases gradually before 50 K, then increases abruptly to a maximum value of 43.35 cm^3 mol^{-1} K at 6 K, and finally decreases to 23.35 cm^3 mol^{-1} K at 2 K, also showing the predominantly ferromagnetic character. The ferromagnetic interaction in **1** is in contrast to the antiferromagnetic interactions observed in the reported Gd_2Ni_4 cluster with the same arrangement of the metal motif.[12] The experimental data were fitted on the basis of the following simplified spin Hamiltonian using the three-J models: $= -2J_1(S_{Ni1}\cdot S_{Ni2A} + S_{Ni1A}\cdot S_{Ni2}) - 2J_2(S_{Ni2}\cdot S_{Gd1} + S_{Ni2}\cdot S_{Gd1A} + S_{Ni2A}\cdot S_{Gd1A} + S_{Ni1}\cdot S_{Gd1} + S_{Ni2A}\cdot S_{Gd1} + S_{Ni2A}\cdot S_{Gd1A}) - 2J_3(S_{Gd1}\cdot S_{Gd1A})$, in which J is the exchange coupling constant between the two ions, as shown in Scheme 1. We used the MAGPACK[20] program, including

Scheme 1. Three-J Model Magnetic Exchange Interactions Employed To Simulate the Susceptibilities of Complex 1

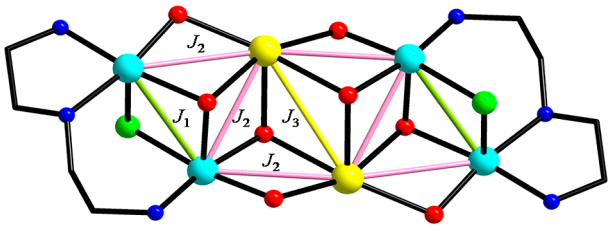

intermolecular interaction (and/or zero-field splitting) by θ value, to model the drop of $\chi_M T$ data at low temperatures. The best-fit parameters for the data were $J_1 = 1.95$ cm^{-1}, $J_2 = -1.46$ cm^{-1}, $J_3 = -0.04$ cm^{-1}, $\theta = -0.06$ cm^{-1}, and $g = 2.22$. The results indicate ferromagnetic interaction between Ni(II) ions, antiferromagnetic interaction between Ni^{II} ions and Gd^{III} ions, and weakly antiferromagnetic interaction within the two Gd^{III} ions. The Gd−Gd and the Ni−Gd coupling are very weak as expected. This simulation study is helpful to understand the magnetic behavior of the species containing anisotropic lanthanide ions, which is much more complicated. The field dependence of the magnetization at 1.9 K appears to be saturated at 7 T to 23.17 μ_B, which is close to the value expected if all the metal ions were in the same direction (22 μ_B).

At room temperature, the $\chi_M T$ values of complexes **2**, **3**, and **4** are 30.24, 34.28, and 34.19 cm^3 mol^{-1} K, respectively. These values are almost in good agreement with the expected theoretical values (**2**: 27.64; **3**: 32.34; **4**: 32.16 cm^3 mol^{-1} K) for two noninteracting lanthanide ions and four uncoupled Ni^{II} ions. Upon cooling, the $\chi_M T$ value increases gradually before 50 K and then increases abruptly to the maximum value of 56.53 cm^3 mol^{-1} K for **2**, 54.72 cm^3 mol^{-1} K for **3**, and 46.52 cm^3 mol^{-1} K for **4** at 7 K, and finally decreases to 20.28, 19.85, and 19.02 cm^3 mol^{-1} K for **2**, **3**, and **4**, respectively, at 2 K. The curve suggests that the couplings within complexes **2**, **3**, and **4** are dominated by ferromagnetic interactions between the paramagnetic centers in the defect-dicubane units. The decrease of the $\chi_M T$ values at low temperature is ascribed to the antiferromagnetic interaction between the spin carriers and the thermal depopulation of the Stark levels of the Tb^{III}, Dy^{III}, and Ho^{III} centers. Compared with the reported Ln_2Ni_4 complexes,[12,13] the direct-current (dc) magnetic measurements indicate that ferromagnetic interaction is dominated in complexes **1**−**5**, while antiferromagnetic coupling for the reported Ln_2Ni_4. The field-dependent magnetization at low temperatures reveals a steady increase approaching the value of 18.79 μ_B for **2**, 22.46 μ_B for **3**, and 20.73 μ_B for **4** at 70 kOe without saturation (Figures S2−S4, Supporting Information). This behavior suggests the presence of magnetic anisotropy and/or the population of low-lying excited states.[21]

Temperature- and frequency-dependent ac susceptibility measurements were carried out under zero dc fields. Strikingly, the results of the ac magnetic susceptibility observed for both Tb-containing and Dy-containing complexes **2** (Figure 5, left) and **3** (Figure 5, right) show that both in-phase and out-of-phase susceptibilities are strongly frequency- and temperature-dependent with a series of frequency-dependent peaks for the out-of phase ac signals (Figure S5, Supporting Information), typical for an SMM. However, only a weak frequency-dependent ac signal below 6 K without peaks in the χ' and χ'' vs T plots, showing the onset of slow relaxation of the magnetization, was observed for the $Ho^{III}_2Ni^{II}_4$ complex **4** (Figure S6, Supporting Information). The out-of-phase (χ'') component of the ac susceptibility of **2** and **3** clearly shows a frequency-dependent peak, respectively. In contrast to what is commonly observed, namely, a decrease of maximum peaks of the χ'' signal upon increasing the temperatures, these peaks increase at the temperature range of the test. These results are striking since most Ni−Ln complexes reported so far do not show SMM behavior under zero dc field.[12−14] Complex **4** does not show similar out-of-phase susceptibility signals with **2** and **3** above 1.8 K under zero dc field. However, the situation is unaltered by the presence of a dc field of 2 kOe for **4**. Such behavior is observed for the first time in the Ni−Tb and Ni−Ho complexes, even though it was previously reported for Ni−Dy systems.[15] No out-of-phase signals were observed for **1** and **5** above 1.8 K.

The blocking temperatures (Tb, Dy maximum of χ'' vs T plot) at 1500 Hz for **2** and **3** are observed at 2.9 and 3.2 K, respectively. The frequency-dependent behavior reveals that the relaxation follows a thermally activated mechanism above 1.9 K, and the plots of $\ln(\tau)$ vs $1/T$ are linear (Figure 6). Fitting the data to the Arrhenius law $[\tau = \tau_0 \exp(U_{eff}/k_B T)]$ afforded an energy barrier of 30 and 32 K for **2** and **3**, respectively, with a pre-exponential factor (τ_0) of $\tau_0 = 2.09 \times 10^{-9}$ and 1.41×10^{-8} s, in line with the expected τ_0 of 10^{-6} -10^{-12} s for an SMM. From these data, Cole−Cole plots of χ'' vs χ' (Figure 6, bottom

dx.doi.org/10.1021/ic402973g | Inorg. Chem. 2014, 53, 3519−3525

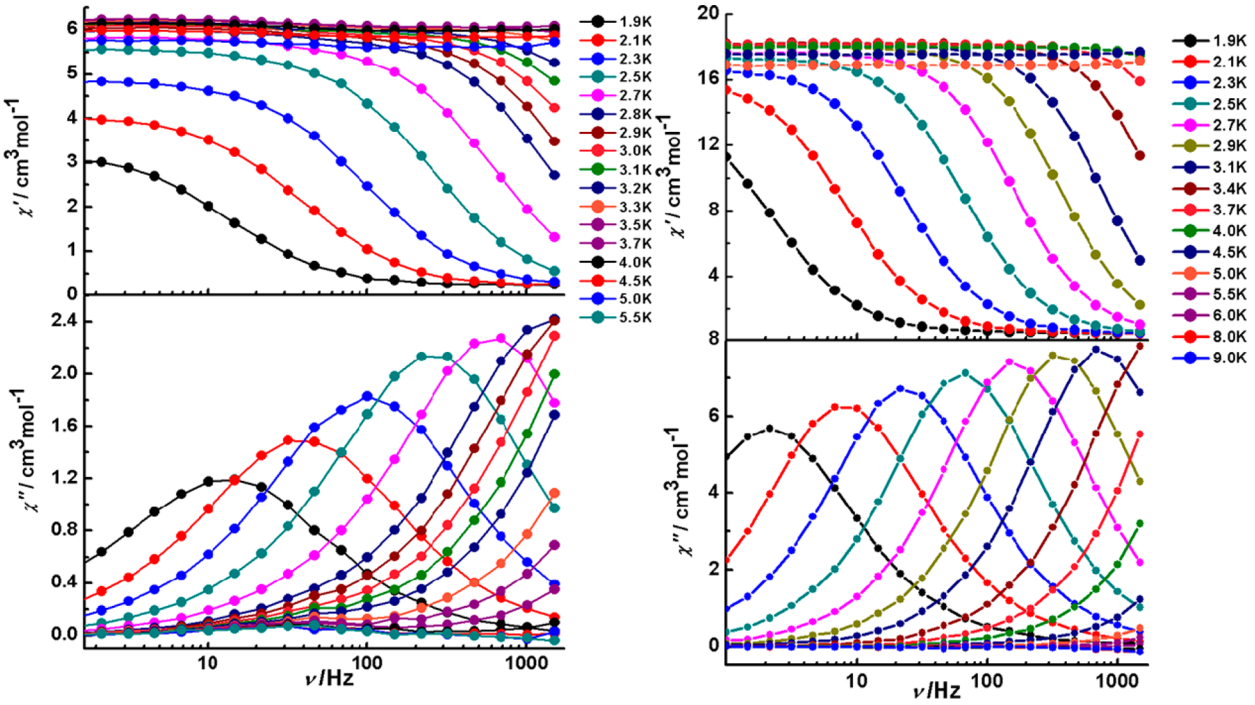

Figure 5. Frequency dependence of the in-phase (χ') and out-of-phase (χ'') ac susceptibilities of **2** (left) and **3** (right) at different temperatures in a zero dc field and a 3 Oe ac field. Solid lines are guides for the eyes.

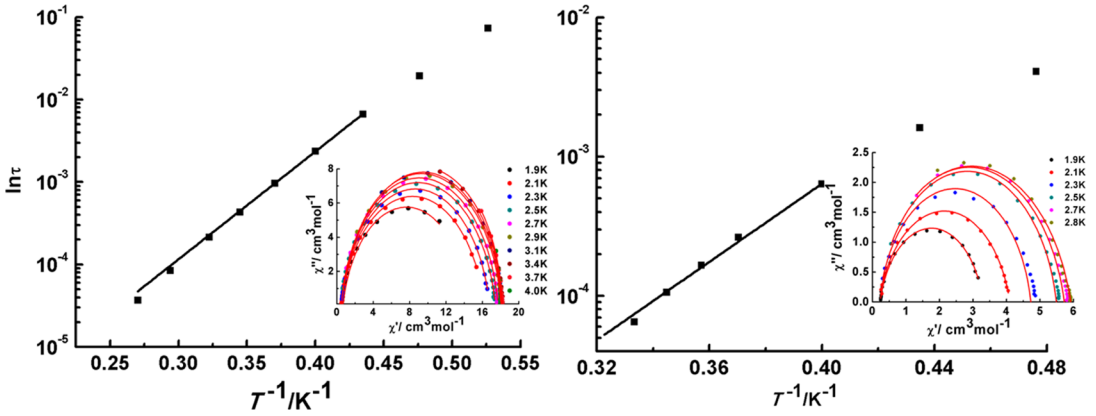

Figure 6. Fitting of the relaxation time (τ) from frequency dependence of the out-of-phase (χ'') parts of the ac susceptibility using Arrhenius law for complexes **2** (left) and **3** (right). Inset: Cole−Cole plots under zero dc field. The solid lines indicate the fits using a generalized Debye model.

inset) can be constructed and fitted to a generalized Debye model[22] to determine α values and relaxation times (τ) in the temperature ranges 1.9−2.8 K for **2** and 1.9−3.1 K for **3**. The relatively symmetrical plots suggest a single relaxation process. The α values, ranging from 0.13−0.16 for **2** and 0.07−0.16 for **3**, indicate a narrow distribution of relaxation times for the single relaxation. All of these magnetic parameters clearly indicate that the remarkable Dy^{III} and Tb^{III} complexes possess SMM nature. This indicates that the d−f polynuclear complex provides a useful design for SMMs due to the high-spin state generated by the frequently observed ferromagnetic interaction between d and f elements and the inherent magnetic anisotropy of the 4f component. Noteworthy, the dynamic magnetic behavior of **2** and **3** is different from that of previously reported Ln_2Ni_4 complexes.[13] Indeed, the literature reported complexes are antiferromagnetically coupled and show only slow magnetic relaxation of magnetization, whereas complexes **2** and **3** with ferromagnetic interaction are found to be SMMs. It is well-established that the magnetic anisotropy of an exchange-coupled system was affected by not only the single-ion anisotropies but also the relative orientation of the local axes.[23] The different coordination environments (eight-coordinated in **2** and **3** and nine-coordinated in the reported Ln_2Ni_4) around the Dy^{III} ion and/or the different relative orientation of the local axes within **2** and **3** and the reported Ln_2Ni_4 are probably responsible for the different relaxation dynamics observed. However, detailed theoretical calculations are required to elucidate the mechanisms operating in polynuclear 3d−4f complexes.

CONCLUSION

In summary, we have successfully obtained five heterometallic Ln−Ni clusters based on the Schiff base ligand H_2L. The core of each structure consists of two distorted $[Ni_2LnO_3Cl]$ defective cubane-like moieties that are further bridged by two hydroxyl groups and two phenolic bridging oxygen atoms to

dx.doi.org/10.1021/ic402973g | Inorg. Chem. 2014, 53, 3519−3525

adjacent cubane, generating a $Ni_4Dy_2O_8Cl_2$ core with two edge-to-edge Ni_2DyO_3Cl defective cubanes. Investigation of their magnetic properties shows ferromagnetic interactions in **1**−**5**. Interestingly, complexes **2** and **3** exhibit SMM characteristics and **4** shows slow relaxation of the magnetization. The absence of frequency-dependent in-phase and out-of-phase signals for the Ni−Y species suggests that the contribution of Ln ions to the anisotropy must be effectual as previously observed in other Ni−Dy samples. However, such a behavior has never been reported in Ni−Tb and Ni−Ho complexes. Efforts to generate new interesting molecules using this ligand and other 3d/4f ions are underway. This synthetic approach represents a promising route toward the assembly of novel 3d−4f clusters and new magnetic materials.

■ ASSOCIATED CONTENT

Ⓢ Supporting Information

Details of the structure solution and refinement (Table S1) and magnetic measurements (Figures S1−S6) for complexes **1**−**5**. This material is available free of charge via the Internet at http://pubs.acs.org.

■ AUTHOR INFORMATION

Corresponding Author

*E-mail: tang@ciac.ac.cn.

Notes

The authors declare no competing financial interest.

■ ACKNOWLEDGMENTS

We thank the National Natural Science Foundation of China (Grants 21201160, 21371166, 21241006, and 21331003) for financial support.

■ REFERENCES

(1) (a) Zhang, J. J.; Sheng, T. L.; Xia, S. Q.; Leibeling, G.; Meyer, F.; Hu, S. M.; Fu, R. B.; Xiang, S. C.; Wu, X. T. *Inorg. Chem.* **2004**, *43*, 5472−5478. (b) Zhuang, G. L.; Jin, Y. C.; Zhao, H. X.; Kong, X. J.; Long, L. S.; Huang, R. B.; Zheng, L. S. *Dalton Trans.* **2010**, *39*, 5077−5079.

(2) Cage, B.; Russek, S. E.; Shoemaker, R.; Barker, A. J.; Stoldt, C.; Ramachandaran, V.; Dalal, N. S. *Polyhedron* **2007**, *26*, 2413−2419.

(3) (a) Bogani, L.; Wernsdorfer, W. *Nat. Mater.* **2008**, *7*, 179−186. (b) Urdampilleta, M.; Klyatskaya, S.; Cleuziou, J. P.; Ruben, M.; Wernsdorfer, W. *Nat. Mater.* **2011**, *10*, 502−506. (c) Moulton, B.; Zaworotko, M. J. *Chem. Rev.* **2001**, *101*, 1629−1658.

(4) (a) Benelli, C.; Gatteschi, D. *Chem. Rev.* **2002**, *102*, 2369−2388. (b) Andruh, M. *Chem. Commun.* **2011**, *47*, 3025−3042.

(5) (a) Leuenberger, M. N.; Loss, D. *Nature* **2001**, *410*, 789−793. (b) Cerletti, V.; Coish, W. A.; Gywat, O.; Loss, D. *Nanotechnology* **2005**, *16*, R27−R49. (c) Timco, G. A.; Faust, T. B.; Tuna, F.; Winpenny, R. E. P. *Chem. Soc. Rev.* **2011**, *40*, 3067−3075. (d) Aromi, G.; Aguila, D.; Gamez, P.; Luis, F.; Roubeau, O. *Chem. Soc. Rev.* **2012**, *41*, 537−546. (e) Hill, S.; Edwards, R. S.; Aliaga-Alcalde, N.; Christou, G. *Science* **2003**, *302*, 1015−1018.

(6) (a) Gatteschi, D.; Caneschi, A.; Pardi, L.; Sessoli, R. *Science* **1994**, *265*, 1054−1058. (b) Sessoli, R.; Tsai, H. L.; Schake, A. R.; Wang, S.; Vincent, J. B.; Folting, K.; Gatteschi, D.; Christou, G.; Hendrickson, D. N. *J. Am. Chem. Soc.* **1993**, *115*, 1804−1816. (c) Liu, J.; del Barco, E.; Hill, S. *Phys. Rev. B* **2012**, *85*, 012406. (d) Murrie, M. *Chem. Soc. Rev.* **2010**, *39*, 1986−1995. (e) Ungur, L.; Chibotaru, L. F. *Phys. Chem. Chem. Phys.* **2011**, *13*, 20086−20090.

(7) (a) Manoli, M.; Collins, A.; Parsons, S.; Candini, A.; Evangelisti, M.; Brechin, E. K. *J. Am. Chem. Soc.* **2008**, *130*, 11129−11139. (b) Evangelisti, M.; Brechin, E. K. *Dalton Trans.* **2010**, *39*, 4672−4676. (c) Evangelisti, M.; Roubeau, O.; Palacios, E.; Camón, A.; Hooper, T. N.; Brechin, E. K.; Alonso, J. J. *Angew. Chem., Int. Ed.* **2011**, *50*, 6606−6609. (d) Langley, S. K.; Chilton, N. F.; Moubaraki, B.; Hooper, T.; Brechin, E. K.; Evangelisti, M.; Murray, K. S. *Chem. Sci.* **2011**, *2*, 1166−1169. (e) Zheng, Y.-Z.; Evangelisti, M.; Winpenny, R. E. P. *Chem. Sci.* **2011**, *2*, 99−102. (f) Sessoli, R. *Angew. Chem., Int. Ed.* **2012**, *51*, 43−45.

(8) (a) Aronica, C.; Pilet, G.; Chastanet, G.; Wernsdorfer, W.; Jacquot, J.-F.; Luneau, D. *Angew. Chem., Int. Ed.* **2006**, *45*, 4659−4662. (b) Sopasis, G. J.; Canaj, A. B.; Philippidis, A.; Siczek, M.; Lis, T.; O'Brien, J. R.; Antonakis, M. M.; Pergantis, S. A.; Milios, C. J. *Inorg. Chem.* **2012**, *51*, 5911−5918. (c) Shiga, T.; Miyasaka, H.; Yamashita, M.; Morimoto, M.; Irie, M. *Dalton Trans.* **2011**, *40*, 2275−2282. (d) Feltham, H. L. C.; Clérac, R.; Powell, A. K.; Brooker, S. *Inorg. Chem.* **2011**, *50*, 4232−4234. (e) Baskar, V.; Gopal, K.; Helliwell, M.; Tuna, F.; Wernsdorfer, W.; Winpenny, R. E. P. *Dalton Trans.* **2010**, *39*, 4747−4750. (f) Abhijeet, K. C.; Biplab, J.; Eric, R.; Guillaume, R.; Sujit, K. G. *Inorg. Chem.* **2012**, *51*, 9159−9161.

(9) (a) Zaleski, C. M.; Depperman, E. C.; Kampf, J. W.; Kirk, M. L.; Pecoraro, V. L. *Angew. Chem., Int. Ed.* **2004**, *43*, 3912−3914. (b) Karotsis, G.; Kennedy, S.; Teat, S. J.; Beavers, C. M.; Fowler, D. A.; Morales, J. J.; Evangelisti, M.; Dalgarno, S. J.; Brechin, E. K. *J. Am. Chem. Soc.* **2010**, *132*, 12983−12990. (c) Saha, A.; Thompson, M.; Abboud, K. A.; Wernsdorfer, W.; Christou, G. *Inorg. Chem.* **2011**, *50*, 10476−10485. (d) Ako, A. M.; Mereacre, V.; Clérac, R.; Wernsdorfer, W.; Hewitt, I. J.; Anson, C. E.; Powell, A. K. *Chem. Commun.* **2009**, 544−550. (e) Xie, Q.-W.; Cui, A.-L.; Tao, J.; Kou, H.-Z. *Dalton Trans.* **2012**, *41*, 10589−10595. (f) Liu, J. Y.; Ma, C. B.; Chen, H.; Hu, M. Q.; Wen, H. M.; Cui, H. H.; Song, X. W.; Chen, C. N. *Dalton Trans.* **2013**, *42*, 2423−2430.

(10) (a) Zhou, Q.; Yang, F.; Liu, D.; Peng, Y.; Li, G. H.; Shi, Z.; Feng, S. H. *Dalton Trans.* **2013**, *42*, 1039−1046. (b) Ferbinteanu, M.; Kajiwara, T.; Choi, K.-Y.; Nojiri, H.; Nakamoto, A.; Kojima, N.; Cimpoesu, F.; Fujimura, Y.; Takaishi, S.; Yamashita, M. *J. Am. Chem. Soc.* **2006**, *128*, 9008−9009. (c) Xu, G.-F.; Gamez, P.; Tang, J.; Clérac, R.; Guo, Y.-N.; Guo, Y. *Inorg. Chem.* **2012**, *51*, 5693−5698. (d) Schray, D.; Abbas, G.; Lan, Y.; Mereacre, V.; Sundt, A.; Dreiser, J.; Waldmann, O.; Kostakis, G. E.; Anson, C. E.; Powell, A. K. *Angew. Chem., Int. Ed.* **2010**, *49*, 5185−5188. (e) Zeng, Y.-F.; Xu, G.-C.; Hu, X.; Chen, Z.; Bu, X.-H.; Gao, S.; Sañudo, E. C. *Inorg. Chem.* **2010**, *49*, 9374−9383. (f) Abbas, G.; Lan, Y.; Mereacre, V.; Wernsdorfer, W.; Clérac, R.; Buth, G.; Sougrati, M. T.; Grandjean, F.; Long, G. J.; Anson, C. E.; Powell, A. K. *Inorg. Chem.* **2009**, *48*, 9345−9355. (g) Schmidt, S.; Prodius, D.; Novitchi, G.; Mereacre, V.; Kostakis, G. E.; Powell, A. K. *Chem. Commun.* **2012**, *48*, 9825−9827.

(11) (a) Chandrasekhar, V.; Pandian, B. M.; Vittal, J. J.; Clérac, R. *Inorg. Chem.* **2009**, *48*, 1148−1157. (b) Mondal, K. C.; Sundt, A.; Lan, Y.; Kostakis, G. E.; Waldmann, O.; Ungur, L.; Chibotaru, L. F.; Anson, C. E.; Powell, A. K. *Angew. Chem., Int. Ed.* **2012**, *51*, 7550−7554. (c) Langley, S. K.; Chilton, N. F.; Ungur, L.; Moubaraki, B.; Chibotaru, L. F.; Murray, K. S. *Inorg. Chem.* **2012**, *51*, 11873−11881.

(12) Liu, B. L.; Liu, Q. X.; Xiao, H. P.; Zhang, W.; Tao, R. J. *Dalton Trans.* **2013**, *42*, 5047−5055.

(13) Ke, H. S.; Zhao, L.; Guo, Y.; Tang, J. *Inorg. Chem.* **2012**, *51*, 2699−2705.

(14) (a) Pasatoiu, T. D.; Etienne, M.; Madalan, A. M.; Andruh, M.; Sessoli, R. *Dalton Trans.* **2010**, *39*, 4802−4808. (b) Colacio, E.; Ruiz-Sanchez, J.; White, F. J.; Brechin, E. K. *Inorg. Chem.* **2011**, *50*, 7268−7273. (c) Cimpoesu, F.; Dahan, F.; Ladeira, S.; Ferbinteanu, M.; Costes, J.-P. *Inorg. Chem.* **2012**, *51*, 11279−11293. (d) Bhunia, A.; Yadav, M.; Lan, Y.; Powell, A. K.; Menges, F.; Riehn, C.; Niedner-Schatteburg, G.; Jana, P. P.; Riedel, R.; Harms, K.; Dehnend, S.; Roesky, P. W. *Dalton Trans.* **2013**, *42*, 2445−2450. (e) Yang, X. P.; Chan, C.; Lam, D.; Schipper, D.; Stanley, J. M.; Chen, X. Y.; Jones, R. A.; Holliday, B. J.; Wong, W.-K.; Chen, S. C.; Chen, Q. *Dalton Trans.* **2012**, *41*, 11449−11453. (f) Polyzou, C. D.; Nikolaou, H.; Papatriantafyllopoulou, C.; Psycharis, V.; Terzis, A.; Raptopoulou, C. P.; Escuer, A.; Perlepes, S. P. *Dalton Trans.* **2012**, *41*, 13755−13764. (g) Xiong, K.; Wang, X.; Jiang, F.; Gai, Y.; Xu, W.; Su, K.; Li, X.; Yuan, D.; Hong, M. *Chem. Commun.* **2012**, *48*, 7456−7458.

(15) (a) Chandrasekhar, V.; Murugesa Pandian, B.; Boomishankar, R.; Steiner, A.; Vittal, J. J.; Houri, A.; Clérac, R. *Inorg. Chem.* **2008**, *47*, 4918−4929. (b) Pasatoiu, T. D.; Sutter, J. P.; Madalan, A. M.; Chiboub Fellah, F. Z.; Duhayon, C.; Andruh, M. *Inorg. Chem.* **2011**, *50*, 5890−5898. (c) Chandra, M. K.; Kostakis, G. E.; Lan, Y.; Wernsdorfer, W.; Anson, C. E.; Powell, A. K. *Inorg. Chem.* **2011**, *50*, 11604−11611. (d) Gao, Y.; Zhao, L.; Xu, X.; Xu, G.-F.; Guo, Y.-N.; Tang, J.; Liu, Z. *Inorg. Chem.* **2011**, *50*, 1304−1308. (e) Pointillart, F.; Bernot, K.; Sessoli, R.; Gatteschi, D. *Chem.—Eur. J.* **2007**, *13*, 1602−1609.

(16) (a) Novitchi, G.; Wernsdorfer, W.; Chibotaru, L. F.; Costes, J.-P.; Anson, C. E.; Powell, A. K. *Angew. Chem., Int. Ed.* **2009**, *48*, 1614−1619. (b) Hosoi, A.; Yukawa, Y.; Igarashi, S.; Teat, S. J.; Roubeau, O.; Evangelisti, M.; Cremades, E.; Ruiz, E.; Barrios, L. A.; Aromi, G. *Chem.—Eur. J.* **2011**, *17*, 8264−8268. (c) Kajiwara, T.; Takahashi, K.; Hiraizumi, T.; Takaisi, S.; Yamashita, M. *CrystEngComm* **2009**, *11*, 2110−2116. (d) Costes, J. P.; Vendier, L. *Eur. J. Inorg. Chem.* **2010**, 2768−2773. (e) Andruh, M.; Costes, J. P.; Diaz, C.; Gao, S. *Inorg. Chem.* **2009**, *48*, 3342−3359.

(17) Long, J.; Habib, F.; Lin, P.-H.; Korobkov, I.; Enright, G.; Ungur, L.; Wernsdorfer, W.; Chibotaru, L. F.; Murugesu, M. *J. Am. Chem. Soc.* **2011**, *133*, 5319−5328.

(18) (a) Zhao, L.; Xue, S. F.; Tang, J. K. *Inorg. Chem.* **2012**, *51*, 5994−5996. (b) Zhao, L.; Wu, J. F.; Xue, S. F.; Tang, J. K. *Chem.—Asian J.* **2012**, *7*, 2419−2423.

(19) (a) Dou, W.; Yao, J.-N.; Liu, W.-S.; Wang, Y.-W.; Zheng, J.-R.; Wang, D.-Q. *Inorg. Chem. Commun.* **2007**, *10*, 105−108. (b) Kong, F.-R.; Zhang, M. *Chem. J. Chin. Univ.* **1999**, *20*, 839−842.

(20) Borrás-Almenar, J. J.; Clemente-Juan, J. M.; Coronado, E.; Tsukerblat, B. S. *Inorg. Chem.* **1999**, *38*, 6081−6088.

(21) Sessoli, R.; Powell, A. K. *Coord. Chem. Rev.* **2009**, *253*, 2328−2341.

(22) (a) Cole, K. S.; Cole, R. H. *J. Chem. Phys.* **1941**, *9*, 341−351. (b) Aubin, S. M. J.; Sun, Z.; Pardi, L.; Krzystek, J.; Folting, K.; Brunel, L.-C.; Rheingold, A. L.; Christou, G.; Hendrickson, D. N. *Inorg. Chem.* **1999**, *38*, 5329−5340.

(23) Bernot, K.; Luzon, J.; Bogani, L.; Etienne, M.; Sangregorio, C.; Shanmugam, M.; Caneschi, A.; Sessoli, R.; Gatteschi, D. *J. Am. Chem. Soc.* **2009**, *131*, 5573−5579.